Changes in the Radial and Tangential Distribution of Radar Reflectivity During Tropical Cyclone Landfalls Over the United States

hurricane.geog.ufl.edu

UF Research Opportunity Fund

Corene J. Matyas and Jingyin Tang, Department of Geography; Markus Schneider, Department of Computer & Information Science & Engineering, University of Florida; Stephanie E. Zick, Department of Geography, Virginia Tech

Contact: Matyas@ufl.edu

Introduction

The primary and secondary wind circulations in a tropical cyclone (TC) help to organize the spatial configuration of its rainbands. For a TC that dissipates after landfall, we expect rainfall to be distributed asymmetrically about the storm center due to differences in friction and moisture availability in the environmental air mass. As TCs interact with the middle latitude westerlies, rainfall should dissipate behind the storm and increase ahead of the circulation center. This study employs Level II data from the Weather Surveillance Radar 1988 Doppler (WSR-88D) network to examine the changing spatial configurations of rainbands in TCs. We employ a new routine for the mosaicking of reflectivity data from multiple radars and convert values into polygons using a Geographic Information System (GIS). We calculate spatial metrics to represent the tangential and radial distribution of reflectivity values in accordance with the primary and secondary wind circulations within the storm. As a TC moves over land, the storm's center should become increasingly exposed to the continental air mass, thereby decreasing the amount of reflectivity values around the circle and decreasing the closure metric. Reflectivity values should become more dispersed as rainfall decreases near the storm center. The rates of exposure and dispersion should differ according to whether the TC completes an extratropical transition (Jeanne 2004) or dissipates after landfall (Humberto 2007).

WSR-88D Reflectivity Processing

- Spline interpolate NHC positions every 5 minutes, hand correct using reflectivity patterns if needed
- Map-reduce framework (Tang and Matyas 2016) to process Level II reflectivity data (Fig. 1)
- Data gridded 250 m x 250 m x 250 m every 5 min using data from a 10-min. window
- Values for cells with multiple values calculated using time-distance weighted function (Lakshmanan et al. 2006) (Fig. 2a)
- Cells with missing values filled via distance-weighted interpolation in GIS (Tang and Matyas 2017)
- Draw contours at 25 and 35 dBZ, run smoothing algorithm, and convert into polygons (Fig. 2b, c)
- Retain polygons with centroids within 500 km of storm center (Fig. 2d)

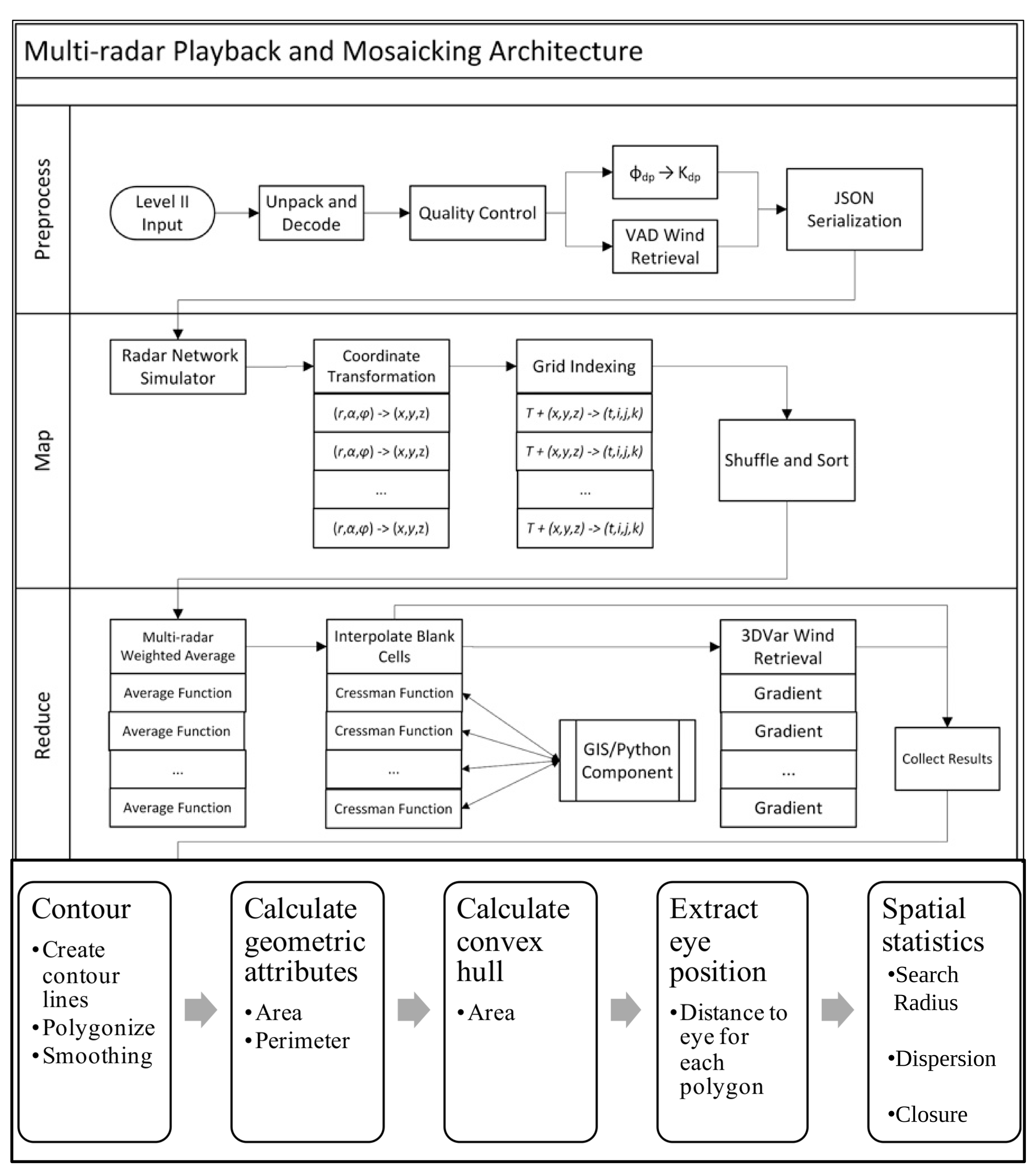

Fig. 1 Procedure to create multi-radar mosaic and spatial analysis in GIS.

Shape Metric Calculations

Metric	Equation	Near 0	Near 1
Dispersion	$D = \sum_{i=1}^{NP} \frac{Area_i}{\sum_j^{NP} Area_j} \left(\frac{r_{centroid,i}}{r_{search}}\right)$	Centralized	Dispersed
Closure	$C = \frac{no.1° \; angles \; intersecting \; polygons}{360}$	Exposed	Enclosed

Dispersion measures the radial distribution of precipitation with respect to the circulation center. This metric increases to a value of unity as the reflectivity region centroid(s) ($r_{centroid}$) (Fig. 2d) move radially away from the circulation center toward the search radius (r_{search}) of 500 km. Each reflectivity region is weighted by its area, with larger regions receiving more weight, and the final metric is calculated by summing over all distinct reflectivity regions, with NP representing the number of polygons (Zick and Matyas 2016, Matyas et al. 2017). Dispersion should increase after landfall.

Closure should decrease after landfall. As TC rainbands tend to curve, we quantify the degree to which the storm center is enclosed by reflectivity values (Matyas 2007, Matyas and Tang 2015, Matyas et al. 2017). We count the number of 1° radials (Fig. 2e) emanating from the circulation center out to 500 km that intersect with a polygon (Fig. 2f) and divide by 360 so that a result of 1 indicates complete closure, while 0.5 indicates that only half of the arc around the TC is filled with reflectivity values.

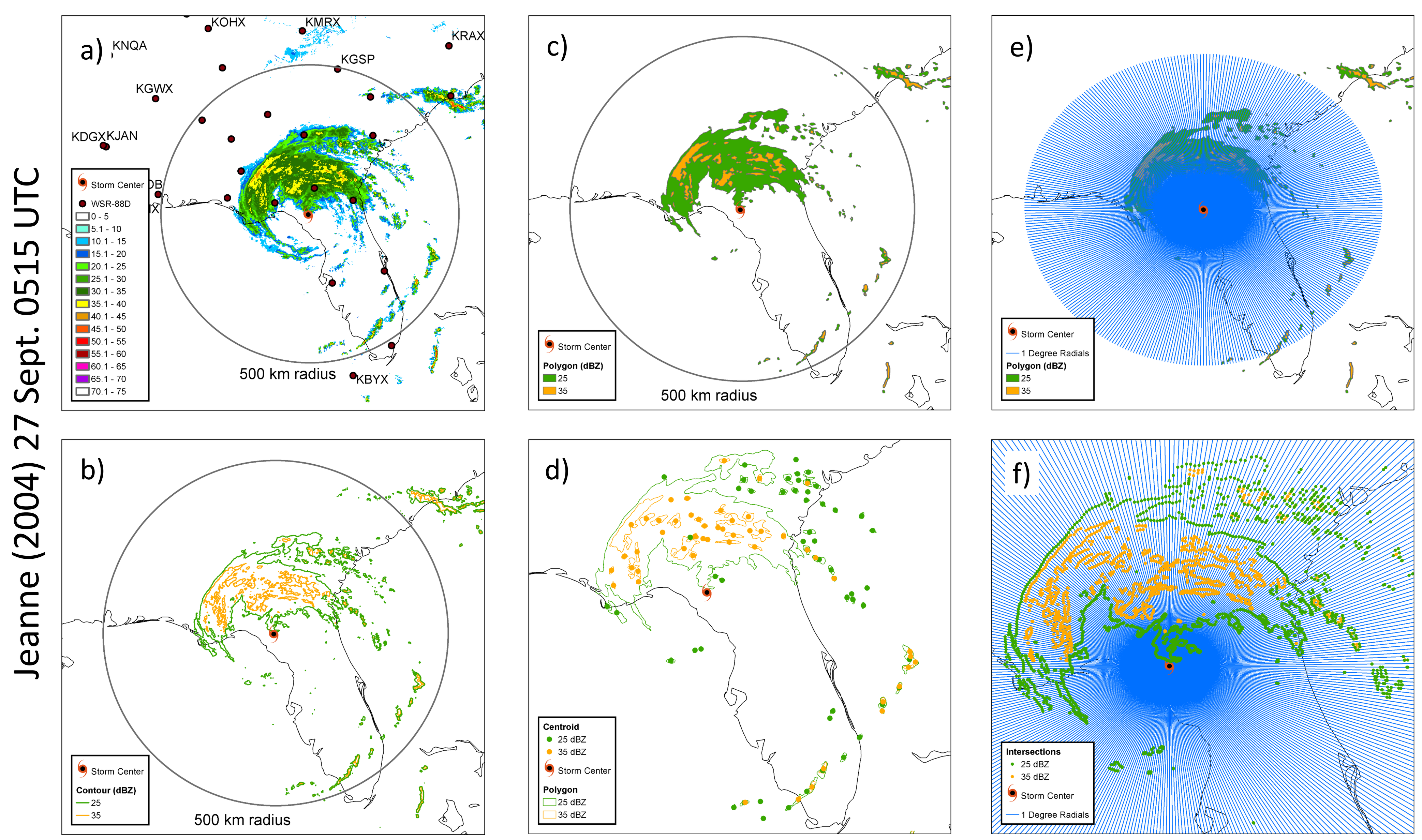

Fig. 2 a) reflectivity mosaic, b) contours of reflectivity, c) contours converted to polygons, d) centroids of polygons for dispersion calculation, e) 1° radial lines in 500 km search radius, f) points of intersection between polygons and radial lines for closure metric.

Results

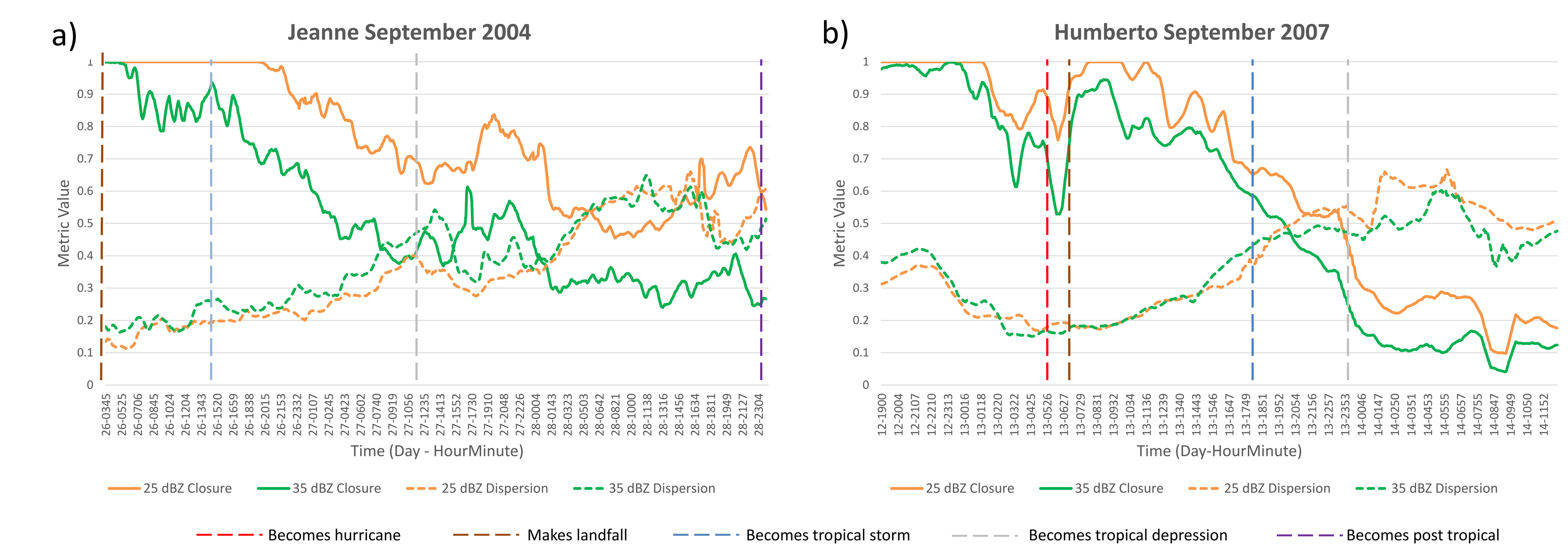

Fig. 3 Closure and dispersion metrics smoothed over a 35-minute window for reflectivity regions of 25 and 35 dBZ.

Jeanne (Franklin et al. 2006) (Fig. 3a)

- Dispersion increased linearly from landfall as rainfall decreased in the core until reaching TD intensity. Then rainfall became more linearly-orientated along a frontal boundary north of center around 1500 UTC on the 27th. The rates of increase were 0.2 over 27 hours for 25 and 0.35 over 34 hours for 35 dBZ.
- Dispersion decreased briefly due to development of a rainband 140 km east of center.
- Dispersion increased more sharply (0.22 in 9.5 hours) as the core eroded and the main region of convection developed 200 km northeast of center, then levelled off as rainfall again stretched linearly north of center along the frontal zone and spine of the Appalachian Mountains.
- 35 dB*Z* exposure began when Jeanne weakened to a TS and 25 dB*Z* began 5 hours later. Closure decreased over a 15-hour period at a rate of 7°per hour.
- Although the inner core continued to be exposed, a 7 (11) hour increase in closure occurred due to development of an outer rainband 400 km east of center.
- Closure increased for 25 dB*Z* as Jeanne merged with a frontal system and became extratropical. The increase was due to a rainband 300 km east of center that lengthened towards the south.

Humberto (Brennan et al. 2009) (Fig. 3b)

- Humberto formed close to shore and was intensifying at landfall, hence rapid changes in shape.
- Rainfall was located mainly east of center while core developed, hence exposed center, but became more centralized as hurricane intensity achieved.
- After landfall, closure decreased by 19° per hour for 12.5 hours, leveling off after weakening to a tropical depression. Rainfall remained east of center during the analysis period.
- Rainfall became more dispersed at a rate of 0.3 over 14 hours, again leveling off after weakening to a tropical depression and with little rainfall remaining in the core.

Conclusions

- Changes in dispersion and closure occur in conjunction with changes in storm intensity.
- Jeanne's interaction with a frontal boundary and topography coincided with brief re-organization.
- Humberto's increases (decreases) in dispersion (closure) occur at constant rate until weakening to TD.
- Dispersion increased from 0.2 to 0.6 in both TCs, but took 48 (24) hours for Jeanne (Humberto).
- Closure in Jeanne (Humberto) decreased by 50 (85)% in 35 (24) hours.
- Correlation coefficients between dispersion and closure averaged -0.87.
- Future work will examine changes in environmental conditions and associations with shape change.

References

Brennan, M. J., R. D. Knabb, M. Mainelli, and T. B. Kimberlain, 2009: Atlantic Hurricane Season of 2007. *Mon. Wea. Rev.*, **137,** 4061-4088.

Franklin, J. L., R. J. Pasch, L. A. Avila, J. L. Beven, M. B. Lawrence, S. R. Stewart, and E. S. Blake, 2006: Atlantic hurricane season of 2004. *Mon. Wea. Rev.*, **134,** 981-1025.

Lakshmanan, V., T. Smith, K. Hondl, G. J. Stumpf, and A. Witt, 2006: A real-time, three-dimensional, rapidly updating, heterogeneous radar merger technique for reflectivity, velocity, and derived products. *Wea. Forecasting*, **21,** 802-823.

Matyas, C. J., 2007: Quantifying the shapes of US landfalling tropical cyclone rain shields. *Professional Geographer*, **59,** 158-172.

Matyas, C. J., and J. Tang, 2015: Measuring gaps in tropical cyclone rainbands using Level II radar reflectivity data. *69th Annual Interdepartmental Hurricanes Conference*, Jacksonville, FL.

Matyas, C. J., S. E. Zick, and J. Tang, 2017: Using spatial metrics to compare observed and simulated reflectivity during the landfall of Hurricane Isabel (2003). *Mon. Wea. Rev.*, **In revision.**

Tang, J., and C. J. Matyas, 2016: Fast playback framework for analysis of ground-based Doppler radar observations using Map-Reduce technology. *J. of Atmos. and Ocean. Tech.*, **33,** 621-634.

Tang, J., and C. J. Matyas, 2017: Arc4nix: A cross-platform geospatial analytical library for cluster and cloud computing. *Computers & Geosciences*, **In revision.**

Zick, S. E., and C. J. Matyas, 2016: A shape metric methodology for studying the evolving geometries of synoptic-scale precipitation patterns in tropical cyclones. *Annals of the Association of American Geographers*, **106,** 1217-1235.